

Ni(III) vs. Ni(II)-thiyl radical: charge-delocalisation in a binuclear Ni(III)Ni(II)-dithiolate complex

Neil D. J. Branscombe,^a Andrew J. Atkins,^a Armando Marin-Becerra,^a Eric J. L. McInnes,^b Frank E. Mabbs,^b Jonathan McMaster^a and Martin Schröder^{*a}

^a School of Chemistry, The University of Nottingham, Nottingham, UK NG7 2RD

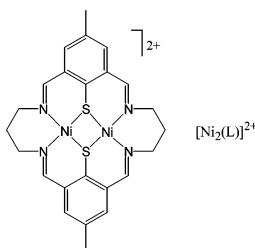
^b EPSRC EPR Service Centre, Department of Chemistry, The University of Manchester, Oxford Road, Manchester, UK M13 9PL

Received (in Cambridge, UK) 9th January 2003, Accepted 18th February 2003

First published as an Advance Article on the web 2nd April 2003

Multi-frequency EPR spectroscopy on ⁶¹Ni-labelled samples of [Ni₂(L)]³⁺ confirms extensive charge-delocalisation between the Ni(III) centre and thiolate donors in the Ni(II)Ni(III) complex.

The crystal structure of [NiFe] hydrogenase from *Desulfovibrio gigas* confirms the presence of a highly unusual binuclear [NiFe] centre (Ni–Fe = 2.9 Å) at the active site.¹ The Ni centre possesses S₄ co-ordination comprising two terminal cysteinates and two cysteinates which bridge to the Fe site which is also bound to a CO and two CN[−] ligands. The redox chemistry of the active site of [NiFe] hydrogenase is particularly rich and at least nine spectroscopically distinct states associated with four redox levels of the enzyme have been identified.² The oxidised, catalytically-inactive Ni-A and Ni-B forms exhibit distinct EPR signals that have been assigned to a formal “Ni(III)Fe(II)” state containing cysteine-thiyl radical character.² Evidence for this redox non-innocence of the cysteinate ligands at the active site of [NiFe] hydrogenase derives from EPR spectroscopic studies on small molecule analogues,³ on the ³³S-labelled enzyme⁴ and on single crystals of [NiFe] hydrogenase from *D. vulgaris*.⁵ Orientation-selected ENDOR spectroscopic studies⁵ on [NiFe] hydrogenase from *Chromatium vinosum* and theoretical calculations also support considerable thiyl radical character in the Ni-B form of the enzyme.⁶



We report herein the degree of electron delocalisation within a formally Ni(III) complex containing bridging thiolate ligation as a measure of the potential redox non-innocence of thiolate donors bound to Ni. This was achieved by a multi-frequency EPR spectroscopic study on the one-electron oxidation product of [Ni₂(L)]²⁺.⁷ This compound offers a unique opportunity to probe the Ni(III) state in the presence of a protected dithiolate bridge and in a geometry about Ni that resembles that of the active site of [NiFe] hydrogenase.⁸

[Ni₂(L)]²⁺ shows a reversible oxidation at $E_{1/2} = +0.55$ V vs. Fc–Fc⁺ assigned to the formation of a formal Ni(II)Ni(III) species.⁹ This assignment, however, is simplistic and does not take into account potential covalency of the Ni–S bond.¹⁰ Coulometric studies confirm the oxidation to be a one-electron process and UV/Vis spectroelectrochemistry at 273 K demonstrates a fully reversible [Ni₂(L)]^{2+/3+} couple. Furthermore, the cyclic voltammogram of chemically prepared [Ni₂(L)]³⁺ [$\lambda_{\text{max}} = 510$ (ε_{max} = 245); 865 nm (85 M^{−1} cm^{−1})] is identical to that of the starting material [Ni₂(L)]²⁺.

The fluid solution X-band EPR spectrum of [Ni₂(L)]³⁺ generated electrochemically in the presence of Bu₄NPF₆ exhibits a single line at $g_{\text{iso}} = 2.155$. However, at S-band and 270 K a 1:2:3:2:1 pentet is resolved, due to hyperfine coupling of the unpaired electron with two equivalent ¹⁴N nuclei ($I = 1$, $a_{\text{iso}}(\text{N}) = 17 \times 10^{-4}$ cm^{−1}). The S-band spectrum of an 86.2% enriched ⁶¹Ni ($I = 3/2$) sample of [Ni₂(L)]³⁺ under identical conditions reveals extra structure due to the ⁶¹Ni hyperfine interaction. Simulation using identical parameters to those determined for the natural abundance sample,¹¹ and with the ⁶¹Ni hyperfine coupling constant as the only variable, gives $A_{\text{iso}}(\text{Ni}) = +5.9 \times 10^{-4}$ cm^{−1}. The positive sign of $A_{\text{iso}}(\text{Ni})$ is determined by simulation of the m_I dependence of the linewidths.¹¹ Significantly, good simulations for this and all other EPR spectra in this work (see below) were only possible assuming hyperfine coupling to *one* Ni centre.

The frozen solution X-band EPR spectrum of [Ni₂(L)]³⁺ is near axial with a well-resolved 1:2:3:2:1 pentet structure in the parallel region, with slight rhombicity in the perpendicular region in addition to hyperfine structure (Fig. 1a). The hyperfine resolution is improved markedly at S-band as expected (Fig. 2a). The spectra at both frequencies can be simulated with $g_x = 2.202$, $g_y = 2.187$, $g_z = 2.035$, with hyperfine coupling to two ¹⁴N with $a_x(\text{N}) = a_y(\text{N}) = 17 \times 10^{-4}$ cm^{−1}, $a_z(\text{N}) = 19 \times 10^{-4}$ cm^{−1} (Figs. 1a and 2a). Extra hyperfine structure is resolved on ⁶¹Ni-enrichment at S- and X-band, and simulations using the same parameters as for the natural abundance spectra gives $A_x(\text{Ni}) = \pm 19 \times 10^{-4}$ cm^{−1}, $A_y(\text{Ni}) = \pm 16 \times 10^{-4}$ cm^{−1} and $A_z(\text{Ni}) = \pm 17 \times 10^{-4}$ cm^{−1} (Figs. 1b and 2b).

The pattern of the g -values $g_x \approx g_y > g_z \approx g_e$ (g_e = the free electron g -value, 2.0023) is indicative of a d_{z^2} ground state where the z axis is perpendicular to the plane of the molecule. In this case the principal values of the g and ⁶¹Ni A -matrices are given by eqns. (1)–(6):¹³

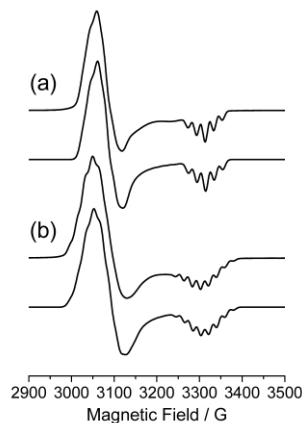


Fig. 1 X-band EPR spectra of [Ni₂(L)]³⁺ in MeCN at 110 K: (a) natural abundance (upper) and simulation (lower) with the parameters in the text; (b) 86.2% ⁶¹Ni enriched (upper) and simulation (lower) with the parameters in the text. Simulations use Gaussian linewidths of $W_x = 17$ G, $W_y = 17$ G and $W_z = 12$ G.

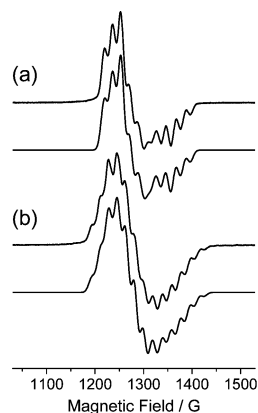


Fig. 2 S-band EPR spectra of $[\text{Ni}_2(\text{L})]^{3+}$ in MeCN 110 K: (a) natural abundance (upper) and simulation (lower) with the parameters in the text; (b) 86.2% ^{61}Ni enriched (upper) and simulation (lower) with the parameters in the text. Simulations use Gaussian linewidths of $W_x = 15$ G, $W_y = 15$ G and $W_z = 12$ G.

$$g_x = g_e - 6\lambda/\Delta_{yz} \quad (1)$$

$$g_y = g_e - 6\lambda/\Delta_{xz} \quad (2)$$

$$g_z = g_e \quad (3)$$

$$A_x = A_s + P[-2a^2/7 + \Delta g_x + \Delta g_y/14] \quad (4)$$

$$A_y = A_s + P[-2a^2/7 + \Delta g_y + \Delta g_x/14] \quad (5)$$

$$A_z = A_s + P[4a^2/7 - (\Delta g_x + \Delta g_y)/14] \quad (6)$$

where $\Delta g_i = g_i - g_e$, A_s is the Fermi contact interaction, λ is the spin-orbit coupling constant for Ni, P is the electron-nuclear dipolar coupling parameter for Ni ($P = -124.3 \times 10^{-4} \text{ cm}^{-1}$), a is the LCAO coefficient of the d_{z^2} orbital in the singly-occupied molecular orbital (SOMO) and Δ_i ($i = xy, xz$) are the energy separations between the ground state and excited states. Eqns. (1)–(6) can be combined to give eqn. (7),¹³

$$A_z - \langle A \rangle = P[4a^2/7 - 17/42(\Delta g_x + \Delta g_y)] \quad (7)$$

where $\langle A \rangle = (A_x + A_y + A_z)/3$. The molecular z axis can be assigned from the pattern of the g -values because $g_z \approx g_e$. Eqns. (4)–(6) imply that A_z should be more negative than A_x or A_y (P is negative). Furthermore, the small magnitude of $A_{\text{iso}}(\text{Ni}) = +5.9 \times 10^{-4} \text{ cm}^{-1}$ implies that one of the anisotropic values must be opposite in sign to the other two and to A_{iso} . Thus we have $A_x = +19 \times 10^{-4} \text{ cm}^{-1}$, $A_y = +16 \times 10^{-4} \text{ cm}^{-1}$ and $A_z = -17 \times 10^{-4} \text{ cm}^{-1}$ ($\langle A \rangle = +6 \times 10^{-4} \text{ cm}^{-1}$).

Solving eqn. (7) with these values gives $a^2 = 0.59$ (taking the opposite signs for all $A(\text{Ni})$ values gives negative values for a^2 , thus supporting our assignments). Thus, the singly occupied molecular orbital (SOMO) is 59% localised in the d_{z^2} orbital of one of the Ni centres. The rest of the unpaired electron density is delocalised over the ligand set, but *not* significantly on the second Ni atom since there is no hyperfine coupling observed to it. The pattern of $a(\text{N})$ values (axial about z) indicates that these couplings may be due to co-ordinated MeCN ligands in the axial positions of the Ni centre, rather than the in-plane ^{14}N nuclei in L. A simple calculation gives the unpaired electron density in each of the ^{14}N orbitals as *ca.* 4%. There is no evidence of further hyperfine coupling to the in-plane ^{14}N nuclei and these couplings must be significantly smaller than the experimental linewidths (15 G).

Thus, a significant proportion (*ca.* 30%) of the unpaired electron density in $[\text{Ni}_2(\text{L})]^{3+}$ must be delocalised onto the

bridging thiolate ligands and **not** onto the second Ni atom. Furthermore, $[\text{Ni}_2(\text{L})]^{3+}$ cannot be viewed as containing a pure “Ni(III)” centre. Rather the charge delocalisation for the Ni–(SR) fragment in $[\text{Ni}_2(\text{L})]^{3+}$ must lie between the $[\text{Ni}^{\text{III}}(-\text{SR})]$ and $[\text{Ni}^{\text{II}}(-\text{SR})]$ redox extremes. This redox non-innocence of thiolate ligands bound to Ni may be very important in controlling the reactivity of the active site of $[\text{NiFe}]$ hydrogenase and suggests that the Ni-A and Ni-B forms of this centre should be viewed as being charge delocalised across one or more of the cysteinyl donors at the active site.

We thank the EPSRC for support. We thank CONACyT and DGAPA-UNAM for support to A. M.-B.

Note and References

- 1 A. Volbeda, M.-H. Charon, C. Piras, E. C. Hatchikian, M. Frey and J. C. Fontecilla-Camps, *Nature*, 1995, **373**, 580; A. Volbeda, E. Garain, C. Piras, A. L. Delacey, V. M. Fernandez, E. C. Hatchikian, M. Frey and J. C. Fontecilla-Camps, *J. Am. Chem. Soc.*, 1996, **118**, 12989; M. Frey, *Struct. Bonding*, 1998, **90**, 98 and references therein; A. L. Delacey, E. C. Hatchikian, A. Volbeda, M. Frey, J. C. Fontecilla-Camps and V. M. Fernandez, *J. Am. Chem. Soc.*, 1997, **119**, 7181.
- 2 J. C. Fontecilla-Camps and S. W. Ragsdale, *Adv. Inorg. Chem.*, 1999, **47**, 283 and references therein; J. C. Fontecilla-Camps, *Struct. Bond.*, 1998, **91**, 1; M. A. Halcrow and G. Christou, *Chem. Rev.*, 1994, **94**, 2421; D. J. E. Spencer, A. C. Marr and M. Schröder, *Coord. Chem. Rev.*, 2001, **219–221**, 1055; M. J. Maroney and R. A. Bryngelson, *J. Biol. Inorg. Chem.*, 2001, **6**, 453.
- 3 M. Kumar, R. O. Day, G. J. Colpas and M. J. Maroney, *J. Am. Chem. Soc.*, 1989, **111**, 5974.
- 4 S. P. J. Albract, A. Kröger, J. W. van der Zwaan, G. Uden, R. Böcher, H. Mell and R. D. Fontijn, *Biochim. Biophys. Acta.*, 1986, **874**, 116.
- 5 Ch. Geßner, M. Stein, S. P. J. Albract and W. Lubitz, *J. Biol. Inorg. Chem.*, 1999, **4**, 379; O. Trofanchuk, M. Stein, Ch. Gessner, F. Lendzian, Y. Higuchi and W. Lubitz, *J. Biol. Inorg. Chem.*, 2000, **5**, 36 and references therein.
- 6 L. de Gioia, P. Fantuca, B. Guigliarelli and P. Bertrand, *Inorg. Chem.*, 1999, **38**, 2658; A. Amara, A. Volbeda, J. C. Fontecilla-Camps and M. J. Field, *J. Am. Chem. Soc.*, 1999, **121**, 4468.
- 7 A. J. Atkins, A. J. Blake and M. Schröder, *J. Chem. Soc., Chem. Commun.*, 1993, 1662; A. J. Atkins, D. Black, A. J. Blake, A. Marin-Becerra, S. Parsons, L. Ruiz-Ramirez and M. Schröder, *J. Chem. Soc., Chem. Commun.*, 1996, 457.
- 8 H. Wang, C. Y. Ralston, D. S. Patil, R. M. Jones, W. Gu, M. Verhagen, M. Adams, P. Ge, C. Riordan, C. A. Marganian, P. Mascharak, J. Kovacs, C. G. Miller, T. J. Collins, S. Brooker, P. D. Croucher, K. Wang, E. I. Stiefel and S. P. Cramer, *J. Am. Chem. Soc.*, 2000, **122**, 10544.
- 9 S. Brooker, P. D. Croucher, T. C. Davidson, G. S. Dunbar, C. U. Beck and S. Subramanian, *Eur. J. Inorg. Chem.*, 2000, 169.
- 10 A. J. Blake and M. Schröder, *Advances in Inorganic Chemistry*, Ed. A. G. Sykes, Academic Press, 1990, **35**, 1; A. J. Blake, R. O. Gould, M. A. Halcrow, A. J. Holder, T. I. Hyde and M. Schröder, *J. Chem. Soc., Dalton Trans.*, 1992, 3427.
- 11 Simulation parameters for fluid solution S-band: $g_{\text{iso}} = 2.155$, $a_{\text{iso}}(\text{N}) = 17 \times 10^{-4} \text{ cm}^{-1}$, Lorentzian linewidth 23 G, $A_{\text{iso}}(\text{Ni}) = +5.9 \times 10^{-4} \text{ cm}^{-1}$ (86.2% ^{61}Ni enriched sample). The linewidths increase from low to high field across this spectrum. This effect, due to incomplete averaging of the hyperfine interaction due to slow tumbling of the microwave frequency, is common and can be modelled as $\Delta H_{\text{pp}} = A + Bm_1$ ($A = 23$ G, $B = 9$ G). If $A_{\text{iso}}(\text{Ni})$ were negative the linewidths would increase from high to low field. For all simulations in this work, spectra of natural abundance and enriched species at a given microwave frequency are simulated using the same set of linewidths and lineshapes. All spectra were recorded and simulated as 1st and 2nd derivatives. Details of the simulation software can be found in reference 12.
- 12 F. E. Mabbs and D. Collison, *Electron paramagnetic resonance of d transition metal compounds*, Elsevier, Amsterdam 1992, Ch. 7.
- 13 A. H. Maki, N. Edlestein, A. Davison and R. H. Holm, *J. Am. Chem. Soc.*, 1964, **86**, 4580.